Biogeosciences

Open Access EGU

# Technical note: Pondi – a low-cost logger for long-term monitoring of methane, carbon dioxide, and nitrous oxide in aquatic and terrestrial systems

**Martino E. Malerba**[1,2], **Blake Edwards**[3], **Lukas Schuster**[1,2], **Omosalewa Odebiri**[2], **Josh Glen**[2], **Rachel Kelly**[2], **Paul Phan**[1,2], **Alistair Grinham**[4], **and Peter I. Macreadie**[1,2]

[1]Centre for Nature Positive Solutions, Department of Biology, School of Science,
RMIT University, Melbourne, VIC 3000, Australia
[2]School of Life and Environmental Sciences, Deakin University, Burwood Campus, Burwood, VIC 3125, Australia
[3]Leading Edge Engineering Solutions Pty. Ltd. (LEES), Yackandandah, VIC 3749, Australia
[4]School of Civil Engineering, The University of Queensland, St Lucia, QLD 4072, Australia

**Correspondence:** Martino E. Malerba (martino.malerba@rmit.edu.au)

**Abstract.** Understanding the complex dynamics of greenhouse gases (GHGs) such as carbon dioxide ($CO_2$), methane ($CH_4$), and nitrous oxide ($N_2O$) fluxes between aquatic and terrestrial ecosystems and the atmosphere requires extensive monitoring campaigns to capture spatial and temporal variations adequately. However, conventional commercial GHG analysers limit data collection due to their high costs, limited portability, cumbersome weight, and restricted field autonomy. To overcome these challenges, we developed the *Pondi* – a lightweight (0.8 kg) logger from cost-effective components tailored for long-term (weeks to months) continuous monitoring of $CO_2$, $CH_4$, and $N_2O$ concentrations in terrestrial and aquatic environments. Components for a *Pondi* cost approximately USD 750 (or AUD 1166) and require 6 h of specialised labour. The *Pondi* features solar panels for indefinite runtime, Global Positioning System (GPS) for tracking, an inertial measurement unit (IMU) for motion detection, and an optional microcontroller-powered add-on to support self-venting and additional sensors. The *Pondi* can be attached to either floating chambers to measure aquatic GHG emissions or terrestrial chambers to quantify respiration (with dark chambers) or net primary productivity (with transparent chambers). The *Pondi* is connected to a cloud-based system for real-time data access and remote configuration. The components for the *Pondi* are readily available in most countries, and basic engineering and IT skills are sufficient to assemble the device. By offering a practical, cost-effective, and reliable solution for GHG monitoring, the *Pondi* contributes to efforts to assess and mitigate anthropogenic GHG emissions.

## 1 Introduction

The continued rise in greenhouse gas (GHG) emissions from human activities is intensifying the impacts of climate change. In 2019, global net anthropogenic emissions reached $59 \pm 6.6\,Gt\,CO_2$-eq, which is a 12 % increase from 2010 and 54 % from 1990 levels (IPCC, 2023). The three dominant GHGs – carbon dioxide ($CO_2$), methane ($CH_4$), and nitrous oxide ($N_2O$) – originate from a range of land- and water-based processes and vary in both atmospheric lifetime and warming potential (EPA, 2023; UN Environment Programme, 2023). Aquatic ecosystems play a critical role in the cycling of all three gases. $CO_2$ is exchanged through aquatic primary production, microbial respiration, and organic matter decomposition (Webb et al., 2019). $CH_4$ is produced in anoxic sediments via methanogenesis and released through diffusion or bubble fluxes (Rosentreter et al., 2021; Saunois et al., 2025). $N_2O$ emissions arise from nitrification and denitrification processes in nutrient-rich waters, including wastewater treatment plants, aquaculture ponds, and agricultural drains (Thakur and Medhi, 2019; Hu et al., 2012). Small

inland waters contribute disproportionately to these fluxes due to high rates of biological activity and large surface-area-to-volume ratios (Holgerson and Raymond, 2016). Yet, quantifying GHG emissions from aquatic systems remains challenging, with large uncertainties arising from spatial heterogeneity, episodic fluxes, and limited monitoring at scale (Rosentreter et al., 2021).

While satellite monitoring and aerial monitoring offer a broad, top-down perspective of GHG emissions, they often fail to capture the fine-scale variability and mechanistic drivers of emissions at the ground level (Boesch et al., 2021). This limitation is particularly problematic in heterogeneous landscapes, such as agricultural mosaics, where GHG sources are spatially variable and often transient (McGinn, 2006). Reliable in situ measurements are essential to overcome this gap, as they provide high-resolution, ground-truth data necessary to calibrate and validate satellite-based and airborne models (Kent et al., 2019; Pigliautile et al., 2020). Ultimately, this synergy between in situ and remote sensing approaches enables more accurate monitoring, supports targeted mitigation strategies, and enhances confidence in large-scale emission inventories (Janssens-Maenhout et al., 2020).

The current landscape of commercial GHG analysers for in situ monitoring has significant limitations (see comparison in Table 1). While accurate and precise, most commercial $CO_2$, $CH_4$, and $N_2O$ analysers have substantial drawbacks in costs, portability, and energy demands (Rodríguez-García et al., 2023). For instance, products from leading companies in this field – such as G2508 and G2509 gas concentration analysers by Picarro, an ultraportable greenhouse gas analyser by Los Gatos Research, and LI-7810 and LI-7815 by Li-COR – are capable of measuring gas concentrations at sub-ppb (parts per billion) levels. However, these devices are expensive, typically $> USD\,50\,000$. They are also heavy, weighing up to 20 kg, and require a power source (e.g. portable generator) to meet their high energy consumption (20–50 W; Rodríguez-García et al., 2023). Alternatively, GHGs can be quantified by sending samples in pre-evacuated vials to a specialised laboratory, eliminating the need to purchase an analyser (Bonetti et al., 2021; Ollivier et al., 2019). However, this approach comes with higher costs per sample, requires personnel in the field for every measurement, and is unsuitable for long-term deployments ($>$ 1 week) because of the risk of gas dissolution and oxidation, leading to underestimation of fluxes (Table 1; Thanh Duc et al., 2020).

Developing loggers for greenhouse gases using cost-effective components is a promising compromise to reduce instrument costs, increase replication, and meet the demand for intensive field campaigns (Table 1). Flux chamber studies, a widely used method in GHG research, involve enclosing a defined area of soil, water, or vegetation to measure gas exchange with the atmosphere. These studies are critical for understanding the spatiotemporal variability in GHG emissions, particularly in ecosystems like freshwater systems, which are significant sources of $CH_4$, $CO_2$, and $N_2O$

(Malerba et al., 2022a, b). Accurate flux chamber measurements provide insights into key processes driving emissions and inform models used for climate change mitigation and policy development (Janssens-Maenhout et al., 2020).

Today, many sensors can be sourced and combined in automatic, lightweight, long-lasting loggers at much lower costs than high-sensitivity commercial models (Bastviken et al., 2020; Dey, 2018; Maher et al., 2019; Morawska et al., 2018; Rodríguez-García et al., 2023; Curcoll et al., 2022; Dalvai Ragnoli and Singer, 2024; Harmon et al., 2015; Sø et al., 2024). While these sensors may lack the sub-ppm (parts per million) accuracy required for direct atmospheric GHG monitoring, they are well suited for flux chamber studies, where gas concentrations increase by orders of magnitude during incubation. This makes them a remarkably cost-effective alternative for capturing accumulation rates within enclosed spaces. Moreover, these sensors can be installed within loggers with standard features like solar panels for indefinite runtime and internet of things (IoT) connectivity to the cloud for real-time data monitoring. However, while many individual components of low-cost, autonomous GHG monitoring are now widely available – such as solar power, cloud connectivity, and off-the-shelf sensors – integrated DIY prototypes that combine all these features into a field-ready, multi-gas logger remain exceptionally rare. Most existing systems are limited to single-gas detection and lack the autonomy and connectivity required for effective field deployment. This gap has created a bottleneck in scaling high-resolution GHG monitoring, especially in regions or applications with limited budgets or technical capacity (Thanh Duc et al., 2020).

This article presents the *Pondi* – a novel open-source IoT device designed to monitor $CO_2$, $CH_4$, and $N_2O$ fluxes (Table 1, Fig. 1). Unlike most existing devices, the *Pondi* is optimised for flux chambers deployed in the field, mounted on either floating chambers to monitor aquatic emissions or terrestrial chambers to monitor emissions from the terrestrial biosphere. This work was motivated by entities like the European Union and the U.S. Environmental Protection Agency being increasingly interested in low-cost GHG monitoring options to improve their capabilities for collecting data in situ at large scales (Borrego et al., 2015; Watkins, 2013).

## 2 Materials

### 2.1 Overview

The *Pondi* is our cost-effective solution for continuous GHG monitoring in aquatic and terrestrial environments (Fig. 1; see Figs. S1–S3 in the Supplement for onboard printed circuit board designs and Table S1 for a list of components). The approximate cost of the components for a *Pondi* is around USD 750 (or AUD 1166) and requires around 6 h of specialised labour to assemble. *Pondi* integrates solar panels to sustain operation indefinitely, with an additional panel avail-

**Table 1.** Comparison of greenhouse gas (GHG) monitoring approaches, including IoT loggers (e.g. *Pondi*), traditional GHG analysers, and manual sampling methods.

| | IoT logger (e.g. *Pondi*) | Traditional GHG analyser | Manual sampling and lab analysis |
|---|---|---|---|
| Cost-effectiveness | Low/intermediate equipment costs (> USD 1000 per unit), low costs per sample | High equipment costs (> USD 50 000 per unit), low costs per sample | Negligible equipment costs, high costs per sample (approx. USD 20 per sample) |
| Accuracy | Sufficient for flux chamber studies | High precision, sub-ppm levels | High precision but risks of gas dissolution and oxidation |
| Deployment | Easy, remote-friendly, solar-powered, self-operating | Logistically challenging, power-hungry, personnel-dependent | Personnel-dependent, unsuitable for long-term deployments |
| Data management | IoT connectivity, cloud-based, real-time monitoring | Varies, often manual data transfer | Manual data transfer after lab processing |
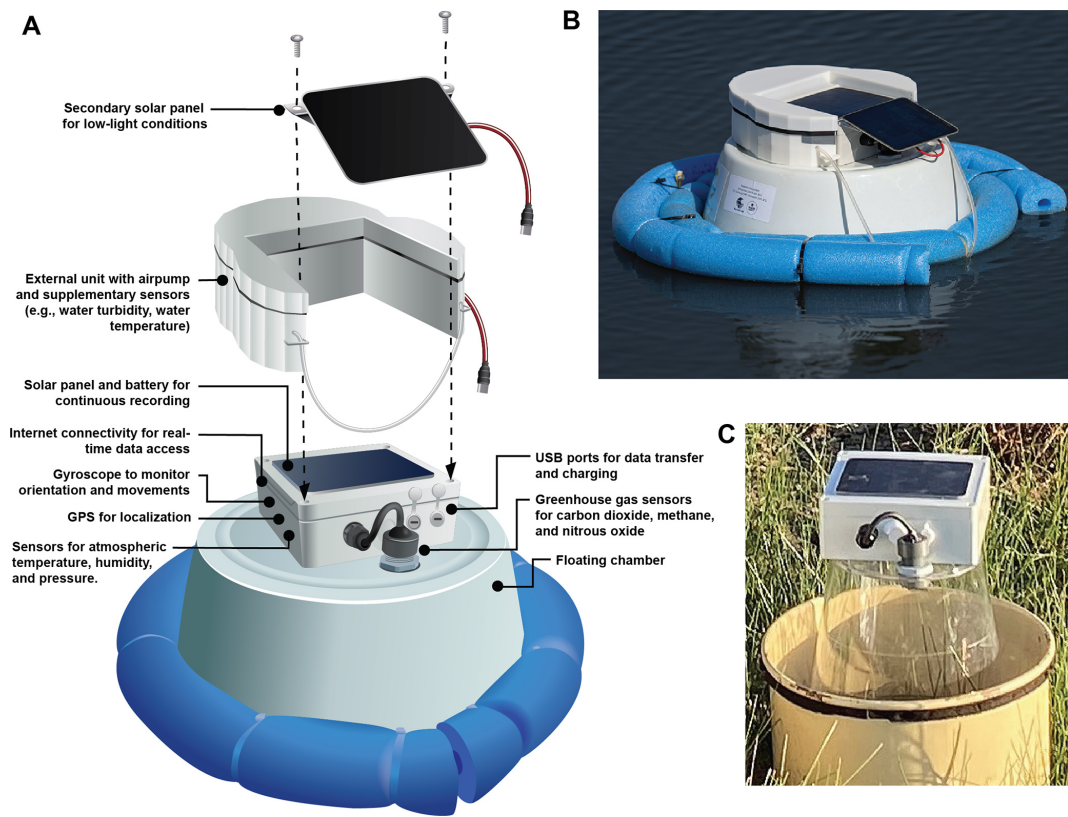


**Figure 1.** *Pondi* logger. **(a)** Device diagram and labels. Photos of *Pondi* during greenhouse gas monitoring of **(b)** a waterbody, including a second solar panel and a secondary unit for periodic self-venting, and **(c)** a terrestrial system mounted on a transparent chamber hermetically sealed inside a metal collar buried in the ground. See Table 2 for details about the gas sensors and Table S1 in the Supplement for a list of components. Image credit: **(b)** Kris Bell, **(c)** Lukas Schuster.

able for improved performance in low-light conditions, such as winter in Melbourne (Australia) with 9 h of sunlight at 2–4 kW h m$^{-2}$ d$^{-1}$ (instead of 15 h at 5–7 kW h m$^{-2}$ d$^{-1}$ in summer). To ensure seamless data management, *Pondi* maintains connectivity to a cloud-based system, reducing reliance on local storage and enabling immediate data access. In case of connectivity loss, *Pondi* transitions to internal storage, initiating a batch data transfer once connectivity is restored. Additional features include GPS for tracking and an inertial measurement unit (IMU) for detecting motion, orientation, and tilt of the device. Finally, *Pondi*'s modular design can connect to an external unit for additional tasks, such as in-

tegrating supplementary sensors (e.g. water turbidity, water temperature) or activating an air pump to reset gas concentrations within the collection chamber to environmental levels.

## Materials and components used

*GHG sensors*. Off-the-shelf sensors measure gas concentrations within the chamber at a user-configurable frequency to calculate fluxes. These sensors are the Figaro TGS2611-E00 for $CH_4$, Sensirion SCD40 for $CO_2$, and Dynament Platinum P/N2OP/NC/4/P for $N_2O$ (see details and URLs in Table 2 and list of the primary components in Table S1). These models were chosen because of their low costs, energy efficiencies, and small sizes. Their detection ranges are 0–10 000 ppm for $CH_4$, 0–40 000 ppm for $CO_2$, and 0–1000 ppm for $N_2O$. Also, they have already been used for field deployment by others (Berthiaume et al., 2020; Demanega et al., 2021; Eugster et al., 2020; Bastviken et al., 2020; Sieczko et al., 2020; Martinsen et al., 2018). The Sensirion SCD40 sensor also measures temperature and humidity, which are used to calculate fluxes and compensate gas readings for these environmental factors (see Sect. 2.5 "Correcting for temperature and humidity").

The *Pondi* supports flexible calibration for each GHG sensor. Users can upload new calibration parameters remotely via the cloud interface, allowing for recalibration without physical access to the device. Following manufacturer guidelines, we performed a one-point calibration for $CH_4$ and $CO_2$ under atmospheric conditions and a two-point calibration for $N_2O$ using both atmospheric concentrations and a high reference concentration (1000 ppm). This architecture enables users to correct for sensor drift over time or to regularly apply new calibrations, which is particularly beneficial for long-term autonomous deployments in remote environments.

Typically, sensors deliver data in digital format directly to the desired units. However, the output of the Figaro $CH_4$ sensor is in analogue format, requiring additional processing to convert these signals into $CH_4$ concentration values. Following Figaro's hardware implementation guide, we incorporated a temperature compensation circuit on our sensor printed circuit board (PCB) using a negative temperature coefficient (NTC) thermistor. Through trial and error, we fine-tuned this circuit over several PCB iterations to minimise the impact of temperature fluctuations on $CH_4$ readings. The *Pondi* reports the Figaro sensor's resistance via a voltage divider, and this resistance is subsequently processed in the cloud to determine $CH_4$ concentration levels. By performing this conversion in the cloud, we can continuously refine and update the equation as calibration data change over time.

Using time series data of gas concentrations measured with *Pondi* sensors, it is possible to estimate the total flux of each gas as

$$F_g(T, P, \mathrm{RH}) = \left( \frac{S_g \cdot C_g(T, P, \mathrm{RH}) \cdot V}{A} \cdot Z_d \cdot Z_g \right), \qquad (1)$$

**Table 2.** Summary of the characteristics of the gas sensors used in the *Pondi*. The "Gas" column indicates the target gas measured. "Sensor Model" lists the specific sensor and its detection technology (e.g. metal oxide or non-dispersive infrared). "Range" provides the operational concentration range validated for field use, while "Res" indicates the resolution, or the smallest detectable change in gas concentration. "Accuracy" refers to the measurement uncertainty at a representative concentration, expressed both in absolute and relative terms. "Cross-Sensitivities" describes known sources of interference, such as temperature, humidity, or other gases. "MAPE" refers to the mean absolute percentage error across a typical measurement range, based on field calibration data. "Notes" explain the strategies implemented to correct or compensate for sensor limitations. Finally, "Ref" provides the source of the information, including manufacturer specifications (with hyperlinks) and peer-reviewed publications. For details on the *Pondi* components, see Table S1. Figaro manual: https://www.figarosensor.com/product/docs/tgs2611-e00_productinfomation(fusa)_rev01.pdf (last access: 16 July 2025). Sensirion manual: https://sensirion.com/media/documents/E0F04247/631EF271/CD_DS_SCD40_SCD41_Datasheet_D1.pdf (last access: 16 July 2025). Dynament manual: https://www.processsensing.com/docs/dynament/tds0132_1.1Platinum-Dual-Range-Non-Certified-Nitrous-Oxide-Sensor-Data-Sheet.pdf (last access: 16 July 2025).

| Gas | Sensor Model | Range | Res | Accuracy | Cross-Sensitivities | MAPE | Notes | Ref (URLs in legend) |
|---|---|---|---|---|---|---|---|---|
| $CH_4$ | Figaro TGS2611-E00 (MOx) | 0–10000 ppm | ∼0.1 ppm | ±1.7 ppm at 28 ppm (ca. 6 %) | Humidity and temperature | 8.93 % (3–10000 ppm) | Temperature correction applied using NTC thermistor. Operating RH usually > 50 %, minimising humidity effects. Minimal temperature and humidity effects (Fig. 4c). | Figaro manual, Shah et al. (2023) |
| $CO_2$ | Sensirion SCD40 (NDIR + T/RH sensor) | 0–40000 ppm | 1 ppm | ±40 ppm at 5000 ppm (ca. 5 %) | Minimal due to NDIR design | 19.9 % (400–10000 ppm) | Integrated temperature and RH compensation. Sensor underpredicts above 5000 ppm (Fig. 3b). | Sensirion manual |
| $N_2O$ | Dynament P/N2OP/NC/4/P (NDIR) | 0–1000 ppm | ∼0.1 ppm | ±50 ppm at 1000 ppm (5 %) | $CO_2$ (∼0.05 ppm $N_2O$ per ppm $CO_2$) | 4.96 % (0–1000 ppm) | $CO_2$ correction factor applied. Sensor robust to temperature and RH variation (Figs. 4a and S7). | Dynament manual |

where $F_g(T, P, \text{RH})$ is the total gas flux ($\text{mg m}^{-2} \text{d}^{-1}$) for the gas $g$ (either $CH_4$, $CO_2$, or $N_2O$); $S_g$ is the rate of change in gas concentration within the chamber over time for each gas ($\text{ppm h}^{-1}$); $V$ is the headspace volume in the chamber ($\text{m}^3$); $A$ is the area of the chamber exposed to the water ($\text{m}^2$); $Z_d$ is the conversion factor from hours to days ($24\,\text{h d}^{-1}$); $Z_g$ is the conversion factor from grams to milligrams ($1000\,\text{mg g}^{-1}$); and $C_g(T, P, \text{RH})$ is the conversion factor from parts per million (ppm) to $\text{mg m}^{-3}$ for each gas, which is calculated based on temperature ($T$), pressure ($P$), and relative humidity (RH) as

$$C_g(T, P, \text{RH}) = \left( \frac{M_g \cdot P_d(T, P, \text{RH})}{R \cdot T} \right). \tag{2}$$

Here $M_g$ is the molecular weight of gas $g$ ($CH_4 = 16.04\,\text{g mol}^{-1}$, $CO_2 = 44.01\,\text{g mol}^{-1}$, $N_2O = 44.013\,\text{g mol}^{-1}$); $R$ is the ideal gas constant ($8.314\,\text{J mol}^{-1}\,\text{K}^{-1}$); $T$ is temperature (in kelvins); and $P_d(T, P, \text{RH})$ is partial pressure of dry air (in Pa), which is calculated as

$$P_d(T, P, \text{RH}) = P - e(T, \text{RH}), \tag{3}$$

where $P$ is total atmospheric pressure and $e(T, \text{RH})$ is the vapour pressure of water at temperature $T$ and relative humidity RH (in %), calculated as

$$e(T, \text{RH}) = \text{RH} \cdot e_s(T). \tag{4}$$

Here $e_s(T)$ is the saturation vapour pressure of water, calculated using the Magnus–Tetens approximation as

$$e_s(T) = 610.78 \cdot \exp\left( \frac{17.27 \cdot [T - 273.15]}{T - 35.85} \right). \tag{5}$$

We explored the sensitivity of Eq. (1) by systematically altering the values of temperature ($T$), atmospheric pressure ($P$), and relative humidity (RH) within the formula, based on typical seasonal variations observed in Victoria (Australia). Specifically, we increased $T$ by 30 °C, decreased $P$ by 10 kPa, and increased RH from 33 % to 99 % while holding all other variables constant. These changes were used to quantify their effect on the calculated gas flux ($F_g$). Results showed that a 30 °C increase in temperature raised $F_g$ by 13 %, a 10 kPa drop in pressure increased $F_g$ by 10 %, and higher relative humidity reduced $F_g$ by 3 % (Fig. S4 in the Supplement).

*Floating or terrestrial chambers*. The *Pondi* uses a sealed chamber to accumulate GHGs. Typically, the *Pondi* is installed on 16 L plastic chambers, but various chamber designs can be used (for details, see Sect. 2.7 "Deployment protocol"). The chamber can be outfitted with flotation rings to monitor aquatic emissions or inserted into the ground for terrestrial flux measurements. In both cases, the chamber must be fully sealed to prevent gas leakage. For terrestrial applications, the chamber is mounted on a 50 cm metal collar

that is driven into the soil to a depth of 5–10 cm. This collar provides structural stability and ensures a hermetic seal between the chamber and the soil surface, minimising diffusion losses during flux measurements. For aquatic applications, the chamber is supported by a custom-designed flotation frame that maintains vertical alignment and ensures the chamber floats stably at the water–air interface, minimising tilting and providing stability even during windy conditions.

The central connection between the *Pondi*'s sensor module and the plastic chamber is established using a threaded plastic screw fitted with an O-ring. This O-ring compresses tightly against the chamber's surface when the screw is secured, creating an airtight seal. Similarly, the $N_2O$ sensor is connected to the chamber via a second hole, using another threaded plastic screw with an O-ring to ensure a secure and leak-free connection (see photos in Fig. S5 in the Supplement). The flux calculations based on changes in gas concentrations are configurable to accommodate different chamber volumes and intake areas.

*Electronics enclosure*. All electronics are incorporated into a waterproof enclosure placed on top of the chamber. A 32 mm hole at the top of the chamber allows the GHG sensors to sample from the chamber space. A 32 mm nut is threaded over the protruding sensors inside the chamber to join the electronics to the chamber securely. The $N_2O$ sensor enters the chamber space separately through a second hole on top of the chamber using the sensor housing offered by the manufacturer (Dynament).

*Power*. Power is provided on board by four 18650 Li-ion battery cells charged through a 2 W solar panel on top of the electronics enclosure. During summer (typically 15 h of sunlight at 5–7 $\text{kW h m}^{-2}\,\text{d}^{-1}$ and max of 120 000 lux), this solar panel provides enough power for the device to monitor gases for at least 4 months every hour or a week every minute. However, in winter (typically 9 h of sunlight at 2–4 $\text{kW h m}^{-2}\,\text{d}^{-1}$ and max of 80 000 lux), the solar panel can power the *Pondi* to monitor gases for 2 weeks at hourly intervals (or a couple of days every minute). For longer deployment, a second 2 W solar panel mounted onto the side of the electronics can extend the total photovoltaic input power during long periods of low sunlight and power the *Pondi* for more than 2 months at hourly intervals (or 2 weeks every minute).

*Connectivity*. An onboard mini peripheral component interconnect express (mPCIe) slot allows connecting to many different off-the-shelf modems. However, the most effective way to connect a *Pondi* is through the 4G Category M1 (CAT-M1) modem, which offers low power and long-range performance and allows data-intensive tasks such as over-the-air (OTA) firmware updates. In remote locations with no CAT-M1 network, the mPCIe slot can support data transfer through a satellite network, although this option will incur higher costs from network providers. Alternatively, in areas

with Wi-Fi availability, the *Pondi* can also be configured for wireless local area network (WLAN) connectivity.

*Onboard microcontroller unit (MCU).* The *Pondi*'s functionality is facilitated by a modern MCU, the ESP32-S3. While a more basic MCU could also be used, the ESP32 enables helpful modern features such as OTA firmware updates and many flexible general-purpose input/outputs (GPIOs) for integrating additional sensors and peripherals.

*Backend data ingestion. Pondi* loggers maintain continuous communications with a cloud provider (i.e. Amazon Web Server, AWS) for uploading telemetry, synchronising device settings, and receiving downlink commands, as well as for various debugging purposes, such as log uploads (Fig. 2). Data from AWS can be used for a frontend website where users can manage device settings and visualise the data received in real time, facilitating efficient data analysis and interpretation. For example, Leading Edge Engineering Solutions (LEES) has developed a frontend using data from AWS to visualise and manage *Pondi* at https://dashboard.leadingedgeengineering.com.au (last access: 15 September 2025) (Fig. 2).

*External self-venting attachment.* To accurately measure GHG emissions over long periods, flux chambers must be periodically reset to ambient conditions to avoid gas saturation. Without venting, gas concentrations inside the sealed chamber can be saturated, leading to an underestimation of emission rates (see Sect. 2.3 "External self-venting attachment with companion microcontroller"). The *Pondi* can be connected to a companion microcontroller to manage the air pump for automatic self-venting. This self-venting attachment is controlled by a control PCB and includes a small 6–12 V direct current air pump with an airflow rate of 1.5–2.0 L min$^{-1}$ through a 5 mm tube (4700 Adafruit Industries LLC; see Table S1 for components). The pump can be initiated for a venting cycle at user-defined intervals (e.g. once a week).

## 2.2 Procedures and data management

The physical components of the *Pondi* logger, including the microcontroller, sensors, communication modules, and power system, are inside the main enclosure. The microcontroller serves as the central processing unit of the *Pondi* logger, coordinating sensor data collection, data processing, and the operation of other components (Fig. 2). It interfaces with various sensors for $CH_4$ (through an analogue-to-digital converter; ADC), $CO_2$, $N_2O$, pressure, temperature, and the inertial measurement unit (IMU). Additionally, it can connect to a companion microcontroller to manage the air pump for automatic self-venting and other sensors for measuring water parameters such as temperature and turbidity.

Once the microcontroller processes the data, it transmits this information to the AWS cloud network via a long-term evolution (LTE) modem (Fig. 2). Alternative transmission

options include satellite or Wi-Fi connectivity. Upon arrival into the network, functions process alerts, check for erroneous data, and generate system health reports. Users access these data via an online web dashboard where they log in to access data and manage settings. This interface allows users to visualise location and time series data of gas concentrations and fluxes ($CH_4$, $CO_2$, and $N_2O$), along with environmental conditions such as temperature, relative humidity, and atmospheric pressure. It also provides insights into onboard analytics, including battery levels, solar panel charging status, and signal strength. Additionally, the device supports remote configuration via the cloud, enabling users to adjust various settings, such as toggling gas and GPS logging, setting logging intervals, configuring air pump flushing frequencies, calibrating sensors, and defining sleep periods to optimise battery usage.

The main enclosure contains the batteries. The device is recharged via solar panel or USB input, with an onboard battery protection system guarding against overcharging, excessive discharge, and other potential risks. The microcontroller monitors the battery state and the flow of charging input to optimise performance by dynamically adjusting the power consumption to suit the conditions.

Additional key features of the onboard logic are listed below.

*Dynamic power usage.* The *Pondi* employs dynamic power management to optimise performance according to available sunlight levels, ensuring efficient energy utilisation. During periods of ample sunlight, power usage is increased to maximise device performance; in low-light conditions, power consumption is minimised to prolong battery life. Key variables governing power usage include the logging rate, upload/reporting frequency, and the duty cycle of sensor heaters. This adaptive approach to power management enables *Pondi* to sustain indefinite operation throughout both summer and winter, facilitated by a single 2 W solar panel in summer and dual 2 W solar panels in winter. The charge sensor monitors the battery's status, optimising power usage and charging cycles, while the charger and battery protection system safeguards against overcharging, discharging, and other potential issues. Finally, the *Pondi* allows the $N_2O$ sensor to be detached when unnecessary, reducing power usage and providing longer battery life.

*Connectivity and onboard storage of offline telemetry.* The *Pondi* is designed to connect with the cloud through the 4G Category M1 (CAT-M1) network to facilitate data offloading immediately after sampling using a commercial data subscription. A SIM card or eSIM with an associated data plan is required for connectivity to this network. This eliminates the need for a separate router or gateway, as the *Pondi*'s onboard modem directly handles data transmission. In remote locations without CAT-M1 coverage, the device can support alternative connectivity options, such as Wi-Fi or satellite internet, by connecting additional modules to the mPCIe slot.
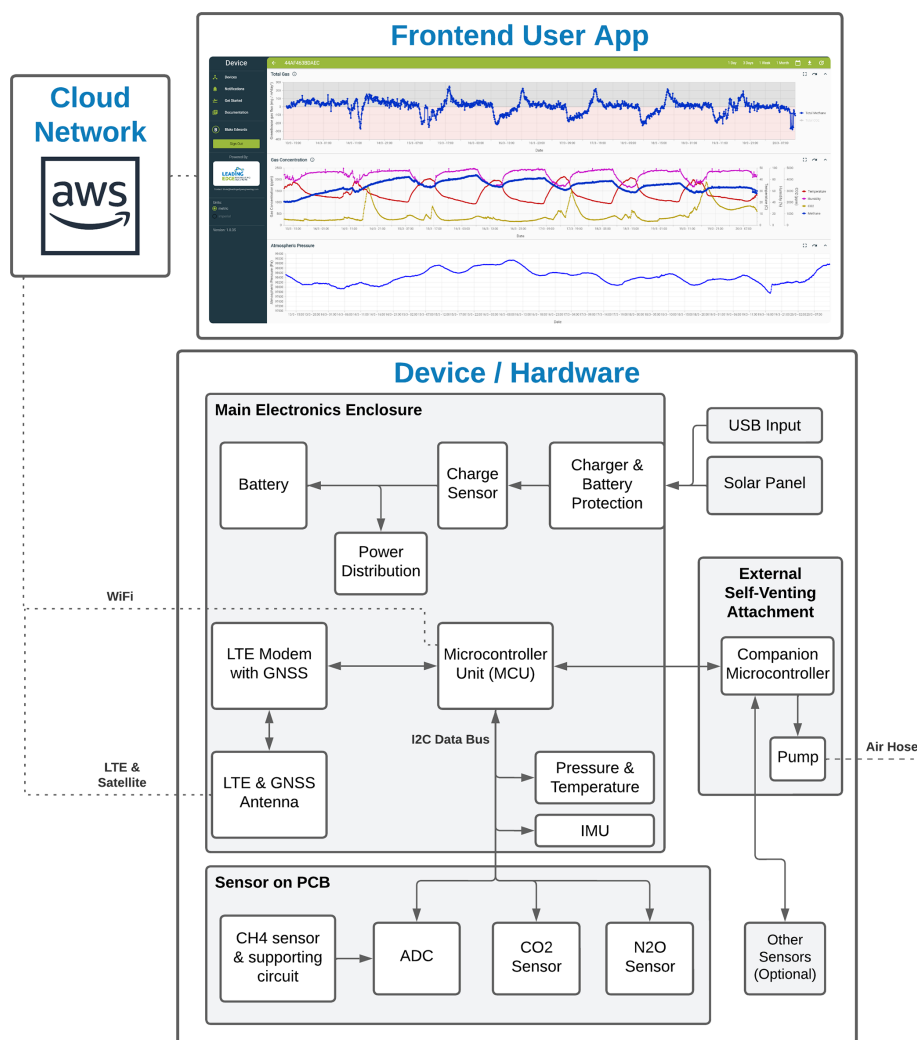
**Figure 2.** Operational logic of the *Pondi* logger. The main enclosure contains the microcontroller, batteries, sensors, and communication modules. The device is powered and recharged through a USB input or a solar panel. It supports connectivity to an external self-venting attachment, which includes a companion microcontroller that controls the automatic air pump and integrates additional sensors. Data from the *Pondi* are transmitted to the cloud via LTE, satellite, or Wi-Fi, enabling real-time monitoring through the frontend user interface.

These features ensure reliable data transfer in a variety of deployment settings. In instances of network unavailability, data packets unable to be transferred to the cloud are stored on board, awaiting reconnection for upload. This logic can also significantly extend battery life by having an upload rate slower than the logging rate. The modem will be powered down in between upload events and will upload multiple stored telemetry packets each time the device is online.

*Movement alerts.* Using the onboard inertial measurement unit (IMU) sensor, *Pondi* can notify users of any changes in its orientation from handling, lifting, or other movements. These alerts serve as convenient markers to indicate the commencement and conclusion of a deployment. Furthermore, they offer insights into external influences, including wind conditions or wildlife interacting with the device – such as birds, mammals, or amphibians.

### 2.3 External self-venting attachment with companion microcontroller

The *Pondi* loggers measure GHG concentrations within a sealed chamber. The concentrations of $CH_4$, $CO_2$, and $N_2O$ inside the chamber rise or fall over time due to release or absorption from soil or water sources. As these gases move between terrestrial or aquatic systems and the air within the sealed chamber, the *Pondi* monitors their concentrations (in ppm) and calculates their flow rates (in $mg\,d^{-1}\,m^{-2}$). However, gas accumulation does not continue indefinitely. Eventually, the gas concentrations reach a point where the emission rate equals the diffusion rate. At this equilibrium point,

known as saturation, the gas levels stabilise, and the emission rates recorded by the *Pondi* loggers no longer represent the typical emissions of a habitat.

For long-term monitoring of aquatic or terrestrial emissions, the system must be vented periodically (typically once a week) to prevent saturation. Manual venting involves temporarily opening the sealed chamber to equalise the air with atmospheric conditions. For automatic venting, the *Pondi* can connect to an external self-venting attachment, which includes a companion microcontroller that controls an air pump to reset the chamber air to atmospheric concentrations. The microcontroller is programmed to initiate the venting process at user-configurable intervals. During each venting cycle, the air pump operates for a set duration (typically 1 h) to flush the chamber with fresh air, ensuring a complete reset to ambient conditions. To prevent pressure buildup inside the chamber, the *Pondi* incorporates a pressure-regulating valve. This valve automatically opens for 10 min following each flushing event, allowing the chamber to equilibrate with atmospheric pressure. This ensures that the system operates under stable conditions and eliminates potential artefacts in gas flux measurements caused by over-pressurisation.

Users can specify the start time, day, and frequency of venting events (e.g. once a week) via the *Pondi*'s cloud-based interface or preset configurations. The algorithm ensures that the venting process aligns with power availability, prioritising periods of sufficient solar energy to recharge the batteries and maintain uninterrupted operation. This automated venting capability enables the *Pondi* to monitor emissions continuously over long-term deployments, minimising the risk of gas saturation while reducing the need for manual intervention.

The companion microcontroller in the external self-venting attachment can also manage additional sensors via a cable extending into the water. These sensors can measure environmental indicators, such as water temperature and turbidity. The companion microcontroller transmits the collected data to *Pondi*'s MCU, preparing them for upload to both the cloud backend and the user-facing application.

## 2.4 Assessment and sensor validation

We validated the $CH_4$ and $N_2O$ sensors within the concentration range specified by the manufacturer: atmospheric levels to 10 000 ppm for $CH_4$ and 0 to 1000 ppm for $N_2O$. Because $CO_2$ accumulation in flux studies often exceeds the range of the *Pondi*'s $CO_2$ sensor (400 to 2000 ppm), we validated its performance outside its specified range (0 to 10 000 ppm). Before validation, we calibrated all sensors using a two-point calibration for $N_2O$ and a one-point calibration for $CH_4$ and $CO_2$ (for details, see Sect. 2.1 "Overview").

We validated the precision and accuracy of all GHG sensors in the laboratory. We created known gas concentrations inside a sealed 15 L plastic water drum (AdVenture Blue Tint Water). For $CO_2$ and $CH_4$, we introduced pure $CO_2$

and $CH_4$ from commercial cylinders using a high-precision fixed flow regulator at 0.25 L min$^{-1}$ (PureGas Aust Pty Ltd). We achieved five concentrations from atmospheric level to 10 000 ppm at 2000 ppm increments by opening the regulator at 14 s intervals. We used a commercial greenhouse gas analyser (UGGA, Los Gatos Research, model 915–0011) to check these concentrations. For $N_2O$, we used three gas cylinders at 0, 500, and 1000 ppm (all balanced with nitrogen gas) to fill the drum and record *Pondi* readings. The drum was kept at 21 °C and away from sunlight. We exposed the *Pondi* to each concentration for 10 min before taking five measurements every 2 min and using the average value.

For each sensor, we calculated the mean absolute percentage error (MAPE) as the average magnitude of percentage errors between predicted ($\hat{y}$) and actual values ($y$), calculated as

$$\frac{1}{n}\sum_{i=1}^{n}\frac{|y_i - \hat{y}_i|}{y_i} \times 100. \tag{6}$$

The $CH_4$ sensor recorded low MAPE (8.93 %), demonstrating high precision and low bias overall (Fig. 3a and Table 2). Only at very high values (ppm > 8000) did the readings show, on average, 10.6 % of systematic overprediction (see points above the 1 : 1 line). The $CO_2$ sensor recorded the highest MAPE (19.9 %; Fig. 3b). It performed well within the concentration range specified by the sensor manufacturers and up to 5000 ppm. Beyond that, the sensor systematically underpredicted readings by on average 21 % (see points below the 1 : 1 line). Finally, the model for $N_2O$ had low MAPE (4.96 %), partly because this sensor has a smaller range (up to 1000 ppm instead of 10 000 ppm; Fig. 3c and Table 2).

## 2.5 Correcting for temperature and humidity

Previous studies have highlighted potential issues with temperature and humidity affecting sensor signals. To address this, we ensured that all sensors included appropriate corrections for these environmental variables. The $CO_2$ sensor (SCD40) features integrated temperature and humidity sensors, enabling real-time compensation across its operating range. Similarly, the $N_2O$ sensor (Dynament Platinum P/N2OP/NC/4/P) incorporates temperature and humidity compensation as part of its non-dispersive infrared (NDIR) technology. In contrast, the $CH_4$ sensor (Figaro TGS2611) lacks built-in corrections and is known to be sensitive to temperature and humidity (van den Bossche et al., 2017; Bastviken et al., 2020). To mitigate this, we implemented a temperature compensation circuit on the printed circuit board (PCB) using a negative temperature coefficient (NTC) thermistor to minimise temperature effects on $CH_4$ readings. For humidity, while dry conditions (relative humidity < 35 %) can compromise $CH_4$ sensor reliability (Eugster and Kling, 2012), the $CH_4$ sensor inside the *Pondi* chamber consistently operates at high humidity levels (50 %–100 %), minimising this concern.
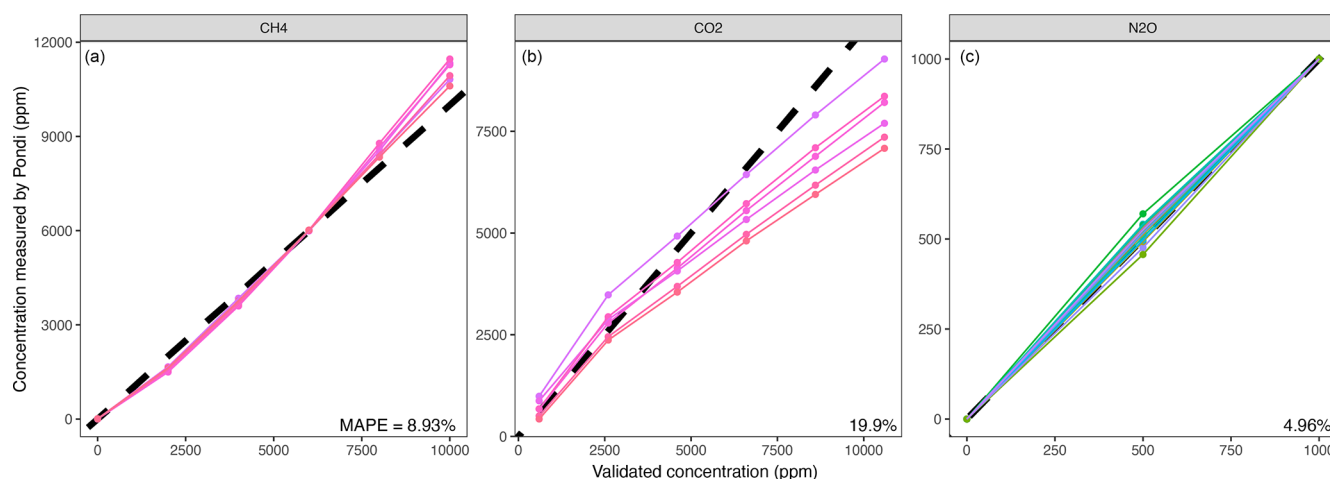
**Figure 3.** Validation of *Pondi* GHG sensors. We tested the $CH_4$, $CO_2$, and $N_2O$ sensors in the *Pondi* at various gas concentrations using gas cylinders in the laboratory. The dashed line represents the unity line (1 : 1 ratio). Each coloured line shows the recordings of a different *Pondi*.

We tested sensor performance for $CO_2$, $CH_4$, and $N_2O$ under controlled laboratory conditions simulating field-relevant temperature and humidity extremes (Figs. 4 and S6 and S7 in the Supplement). Three *Pondi* loggers were placed sequentially in a heated room and a refrigerator to create two scenarios: hot and humid (36 °C, 75 % RH) and cold and dry (15 °C, 50 % RH). These conditions reflect the typical range encountered in mid-latitude field deployments. However, future work will include validation under more extreme temperature and humidity regimes, particularly to support applications in tropical and arid environments. Once temperature and humidity reached equilibrium (see shaded regions in Fig. S6), we recorded mean gas concentrations to evaluate sensor accuracy across both extremes.

Results showed that $N_2O$ readings remained consistent across both conditions ($F_{1,4} = 0.139$, $p = 0.73$; Fig. 4a). $CO_2$ readings exhibited a 7 % decrease under cold and dry conditions ($F_{1,4} = 7.85$, $p = 0.048$; Fig. 4b). $CH_4$ readings showed no statistically significant differences ($F_{1,4} = 2.08$, $p = 0.22$), though there was a slight 3 % decrease in colder and drier conditions (Fig. 4c). These findings demonstrate that temperature and humidity effects on *Pondi* readings are minimal and unlikely to influence estimates in chamber flux studies, where gas concentrations typically increase several-fold. Furthermore, these results align with the precision and accuracy estimates for these sensors (cf. Fig. 3).

## 2.6 Correcting for cross-sensitivities

The manual of the Dynament Platinum $N_2O$ sensor highlights potential cross-sensitivity with $CO_2$, necessitating an approach to account for this effect (Table 2). We used six *Pondi* units across two relative humidity levels (medium at 50 % and high at 70 %) to test how increasing $CO_2$ concentrations might generate false readings for $N_2O$. The re-

sults revealed a consistent spurious increase of 0.05 ppm ($\pm 0.002$ SE; $F_{1,22} = 706$, $p < 0.001$) in $N_2O$ readings per ppm of $CO_2$, regardless of humidity levels (Fig. 5). To address this, we applied a correction factor based on this relationship to the $N_2O$ data.

The $CO_2$ sensor operates using non-dispersive infrared (NDIR) technology, which is intrinsically less susceptible to cross-sensitivities than electrochemical sensors (Table 2). Based on manufacturer specifications and our validation tests, $N_2O$ does not interfere with $CO_2$ detection in this configuration. Additionally, elevated $CO_2$ concentrations had no measurable impact on $CH_4$ readings (Fig. 5).

Outdoor testing demonstrated that the $N_2O$ sensor maintained stable and accurate readings across a broad range of environmental conditions over several weeks. When deployed in a clean plastic bucket filled with rainwater and left outdoors, the *Pondi* consistently reported steady $N_2O$ concentrations, with no detectable influence from fluctuating weather conditions such as temperature, humidity, or solar exposure.

However, it is important to note that accurately resolving small $N_2O$ fluxes remains challenging due to the large relative magnitude of the $CO_2$ cross-sensitivity. Given background concentrations of $\sim 400$ ppm for $CO_2$ and $\sim 0.35$ ppm for $N_2O$, a modest increase in $CO_2$ (e.g. from 400 to 800 ppm) would generate a correction of $\sim 20$ ppm for $N_2O$ (400 ppm $\times 0.05$). With the current uncertainty in the correction coefficient of 4 % (i.e. 0.002/0.05), the resulting error is $\pm 0.8$ ppm $N_2O$ – more than twice the ambient background concentration. This imposes a lower limit of detection that may preclude reliable $N_2O$ flux measurements in natural, low-emitting systems. Nonetheless, the system remains appropriate for high-emitting environments, such as
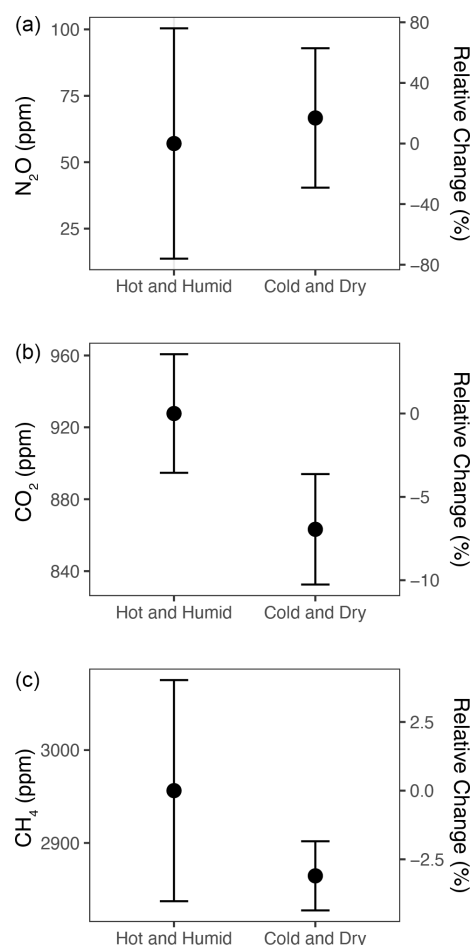
**Figure 4.** Impact of environmental conditions on gas sensor readings, comparing hot and humid conditions (36 °C, 75 %) with cold and dry conditions (15 °C, 50 %). Means and confidence intervals are based on data from three *Pondi* units after reaching equilibrium. Refer to Figs. S6 and S7 for detailed time series of all measured parameters during the trial.

wastewater treatment plants, where background concentrations and fluxes are orders of magnitude larger.

## 2.7 Deployment protocol

*Pondi* loggers must be connected to sealed chambers to monitor the accumulation of greenhouse gas fluxes. These flux chamber studies can happen in aquatic or terrestrial systems, and several deployment protocols are possible. Below, we describe our typical setup for aquatic and terrestrial deployments.

### Aquatic systems

We installed *Pondi* atop a floating chamber to monitor GHG emissions of aquatic systems (Fig. 1b). Before deployment, we activated the logging function through the frontend user app, typically recording data hourly for several weeks. The

*Pondi* was carefully placed on the water surface and gently manoeuvred several metres from the shoreline. We anchored the *Pondi* either by tethering with a rope and a 500 g lead sinker or by installing a pulley system spanning the waterbody, facilitating controlled offshore positioning. In areas with high bird activity such as farm dams, we recommend adding a transparent plastic sheet above the solar panels to shield them from bird droppings (see example in Fig. 6a).

### Terrestrial systems

We embedded a 50 cm metal collar 5–10 cm into the soil. An hour later, we affixed a 10 L plastic transparent chamber inside the metal collar using rubber gaskets to ensure a hermetic seal (Fig. 1c). The *Pondi* was on top of the transparent chamber to monitor gas accumulation. To record carbon fluxes while permitting photosynthesis, the transparent chamber was exposed to natural sunlight, with concurrent measurements of temperature and light intensity. For monitoring dark respiration, the chamber was shielded from light using insulation material. Before switching from dark to light measurements, we flushed the gas collection chamber to restart from atmospheric conditions. Dark and light measurements were typically recorded at 1 min intervals for 30 min. Recording light intensity and temperature outside the *Pondi* and plant biomass inside the chamber offered valuable data for understanding patterns in dark and light respiration.

## 3 Results and discussion

Here, we present and discuss the results of three case studies in which we used *Pondi* to measure concentrations and fluxes of $CO_2$, $CH_4$, and $N_2O$ in different settings, including agricultural ponds, wastewater lagoons, and freshwater wetland systems.

### 3.1 Case study 1: agricultural ponds

Small freshwater systems significantly contribute to the uncertainty in global $CH_4$ budgets (Saunois et al., 2025). This uncertainty partly stems from a lack of data at large spatiotemporal scales necessary to capture the main drivers, such as light, temperature, and rainfall (Naslund et al., 2024; Bastviken et al., 2020). Additionally, short-term monitoring of aquatic habitats often underestimates fluxes by neglecting $CH_4$ ebullition – sporadic releases of $CH_4$ bubbles from sediments – which is a major emission source (Grinham et al., 2018).

Agricultural ponds (also known as farm dams, impoundments, dugouts, or excavated tanks) are waterbodies used in agriculture for irrigation and livestock (Malerba et al., 2021). They are significant sources of GHGs, emitting more per area than many freshwater systems (Grinham et al., 2018; Ollivier et al., 2018). This emission results from the decomposition of organic matter, influenced by temperature, water
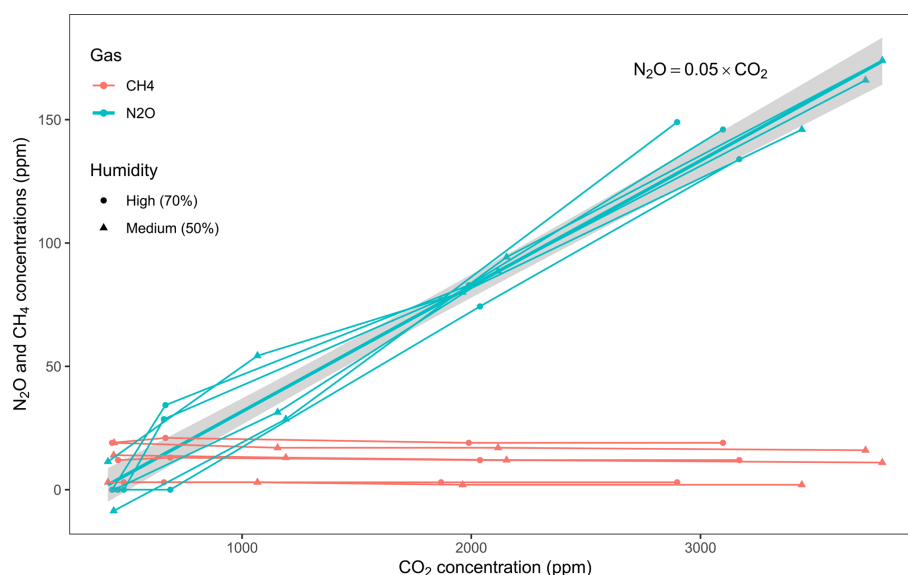
**Figure 5.** Testing the cross-sensitivity of $CH_4$ and $N_2O$ concentrations with increasing $CO_2$ levels. While $CH_4$ was insensitive to $CO_2$, $N_2O$ readings increased by 0.05 ($\pm0.002$ SE) ppm per ppm of $CO_2$, regardless of humidity levels.
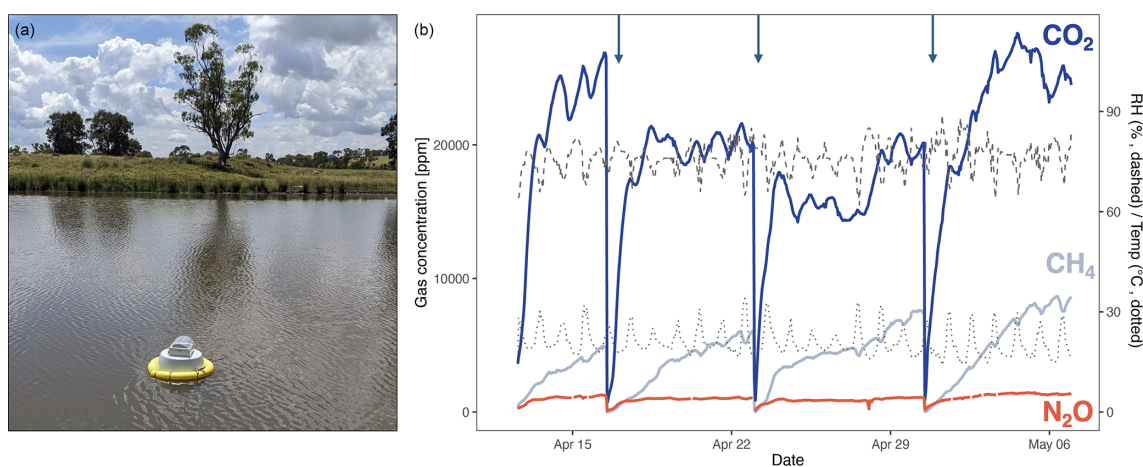


**Figure 6. (a)** *Pondi* in a farm dam. **(b)** 4 weeks of hourly $CO_2$, $CH_4$, $N_2O$, relative humidity (RH), and temperature measurements inside the floating chamber of a *Pondi* in a farm dam. The arrows indicate the three venting events when the air pump diluted gas concentrations by injecting fresh air into the chamber. Image credit: **(a)** Pawel Waryszak.

level changes, and the presence of nutrients and organic matter (Malerba et al., 2022c). The typical time series of GHG fluxes from farm dams shows rapid increases in $CO_2$, reaching saturation after 2–3 d at around 10 000 to 20 000 ppm (Fig. 6). For $CH_4$, the concentration typically increases linearly for around a week until becoming saturated at around 5000 to 10 000 ppm (Fig. 6).

The deployment of *Pondi* in farm dams addresses significant logistical and methodological challenges in monitoring GHG fluxes in small agricultural waterbodies. These devices can monitor multiple sites for long periods, capturing both ebullitive (sudden release of gas bubbles) and diffusive (gradual release) fluxes to better inform us about average emis-

sions and environmental drivers. For example, Odebiri et al. (2024) used *Pondi* to continuously monitor $CH_4$ and $CO_2$ for 3 months in 20 agricultural ponds in Victoria, Australia. This study analysed seasonal drivers to conclude that fencing farm dams to exclude livestock could reduce $CH_4$ emissions by 72 %–92 %. Moreover, the simple design of *Pondi*, combined with geolocation and cloud connectivity, opens up opportunities for citizen science programmes. For example, farmers could receive a *Pondi* and only have to put it in the water to start data collection. This approach could further enhance the cost-effectiveness of documenting GHG fluxes at larger scales without relying on field technicians.

## 3.2 Case study 2: wastewater lagoon

Wastewater treatment plants (WWTPs) emit significant quantities of GHGs, including $CO_2$, $CH_4$, and $N_2O$ (Nguyen et al., 2019). Wastewater typically contains high organic loads and nutrient concentrations, especially nitrogen and phosphorus (Carey and Migliaccio, 2009). These high nutrient concentrations create ideal conditions for microbes to produce $CH_4$ through methanogenesis and $N_2O$ through nitrification and denitrification (Li et al., 2021b). According to IPCC estimates, global GHG emissions from WWTPs account for approximately 2.8 % of total anthropogenic emissions (IPCC, 2007). However, these figures are highly uncertain because they have been estimated using average emission factors from WWTPs worldwide (IPCC, 2007).

Long-term deployments of *Pondi* loggers in wastewater treatment plants (WWTPs) enable precise quantification of anthropogenic GHG emissions at multiple locations. For example, $CO_2$ and $N_2O$ concentrations monitored by a *Pondi* deployed in a wastewater lagoon rose rapidly, reaching saturation within a day (Fig. 7). In contrast, $CH_4$ accumulated more gradually, becoming saturated after approximately 1 week. To continue measuring emission patterns, we vented the chamber weekly to reset gas concentrations to ambient atmospheric levels (Fig. 7).

## 3.3 Case study 3: terrestrial fluxes

Measuring GHG fluxes from terrestrial habitats is essential to understanding their role in carbon sequestration, which is influenced by both abiotic and biotic factors (Smith et al., 2014; Rodrigues et al., 2023; Wu et al., 2023). Restoring degraded ecosystems has become a critical nature-based solution to mitigate climate change by enhancing carbon storage and biodiversity (Houghton et al., 2015; Griscom et al., 2017; Schuster et al., 2024).

Flux measurements using *Pondi* can help in understanding the GHG balances in terrestrial ecosystems and evaluating the effectiveness of ecological restoration. Restoration sites are often remote and difficult to access, making the *Pondi's* small, lightweight design ideal for easy transportation. Additionally, the design of this logger supports various gas collection chambers to measure different types of GHG fluxes. For example, covering the chamber with insulation material or using a dark chamber allows the measurement of $CO_2$ emissions from ecosystem respiration (dark measurement; Fig. 8a). In contrast, clear chambers can estimate net ecosystem exchange (NEE), which accounts for both $CO_2$ emissions and uptake through photosynthesis (light measurement; Fig. 8b).

To measure terrestrial fluxes, there are biological constraints when enclosing vegetation in the chamber for extended durations. Specifically, plants show signs of heat stress, especially when sunlight is allowed to penetrate the transparent chamber. The heat buildup inside the sealed chamber can compromise their physiological functions and introduce inaccuracies into gas exchange measurements. To mitigate this, we limited the duration of terrestrial flux measurements to short intervals (typically $< 30$ min), ensuring that plant metabolism remained stable (i.e. linear trends in $CO_2$ concentrations) and avoiding potential artefacts in the data. Active temperature regulation or intermittent venting might extend the measurement duration while minimising heat accumulation and maintaining plant health.

## 3.4 Limitations and further work

Several opportunities exist to enhance *Pondi* loggers for GHG monitoring: (1) long-term deployments require regular upkeep, typically monthly, to clean solar panels and remove biofouling in aquatic systems. Monthly visits provide a natural opportunity to perform routine recalibration, which helps minimise any long-term drift that might otherwise accumulate. However, adding automatic wipers (such as those for underwater cameras and sensors) could reduce maintenance and extend deployment periods. (2) Adverse weather may cause the *Pondi* to tip, disrupting GHG capture. Improving chamber design for increased stability could minimise this risk. (3) Current sensors in the *Pondi* do not match the accuracy and precision of commercial analysers, especially for $N_2O$ measurements in low-emitting systems. Technological advancements could yield low-cost sensors with higher precision and reduced calibration needs. For example, the modern Sensirion SCD40 used in the *Pondi* has significantly advanced $CO_2$ sensor technology, offering higher accuracy and precision at lower costs and smaller sizes than older models (e.g. SenseAir S8, COZIR Ambient $CO_2$ Sensor, Telaire T6615). (4) The *Pondi* does not include a fan to mix air in the chamber, as adding one would significantly reduce energy efficiency for long-term deployments. While air mixing has not been an issue in our observations, particularly for aquatic applications, future work could evaluate the benefits of integrating a low-energy fan for terrestrial setups. (5) The high-frequency sampling capabilities and venting mechanism of the *Pondi* enable the potential separation of total methane fluxes into their two primary components: diffusive (slow, continuous transport of $CH_4$ across the air–water interface) and ebullitive (episodic release of $CH_4$ bubbles from sediments) fluxes. Although we have not yet conducted this analysis, published methodologies that detect temporal discontinuities in $CH_4$ concentration data are well suited for application to *Pondi* data (Hoffmann et al., 2017; Varadharajan and Hemond, 2012).

## 4 Comments and recommendations

Scalable, low-cost, IoT technology, such as the *Pondi*, can revolutionise our understanding of carbon and nitrogen cycles by reducing costs and overcoming the logistical chal-
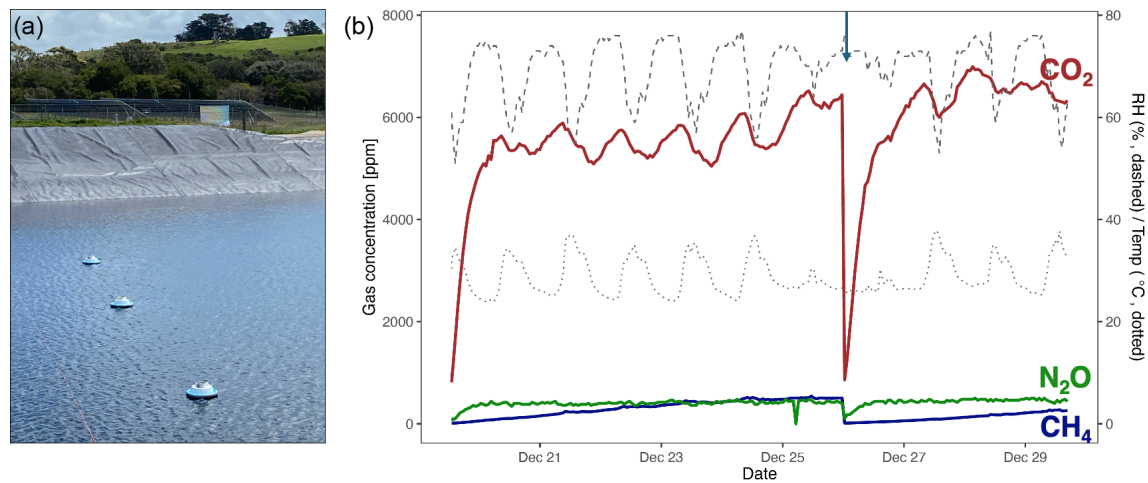
**Figure 7. (a)** Three *Pondi* units in a wastewater lagoon. **(b)** 10 d of hourly $CO_2$, $CH_4$, $N_2O$, relative humidity (RH), and temperature measurements inside the floating chamber of a *Pondi* in a wastewater lagoon. The arrow indicates the venting event when the air pump diluted gas concentrations by injecting fresh air into the chamber. Image credit: **(a)** Lukas Schuster.
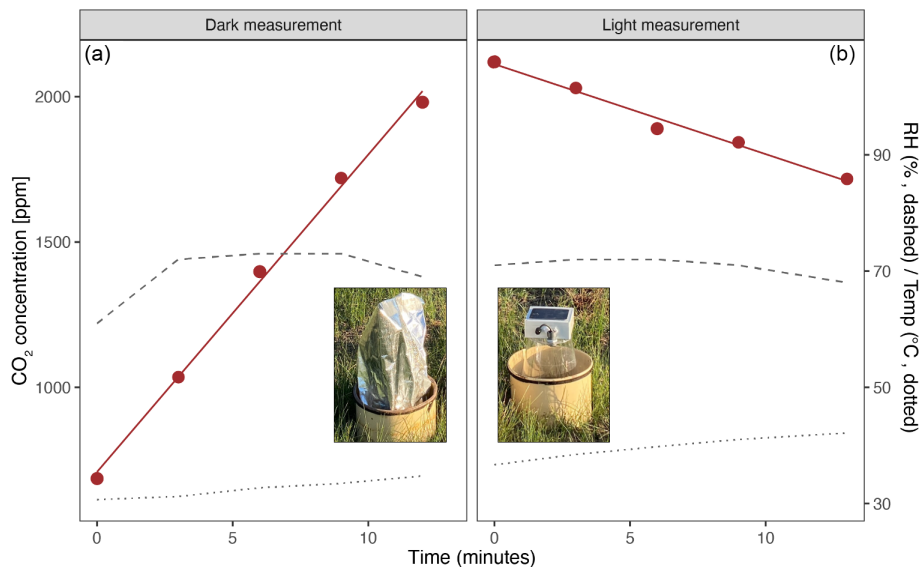


**Figure 8.** Monitoring $CO_2$ concentrations in vegetated terrestrial systems using *Pondi*. **(a)** *Pondi* recording dark respiration after the transparent chamber is covered with insulation material. **(b)** *Pondi* recording net primary production by allowing light through a transparent chamber. Coloured dots are measurements from a *Pondi*. Continuous coloured lines are linear models to estimate emission rates (dark measurement) and sequestration (light measurement). Dashed and dotted lines are relative humidity (RH) and temperature measurements inside the chamber of the *Pondi*, respectively. Image credit: Lukas Schuster.

lenges of collecting data from the field (Salam, 2024; Li et al., 2021a). These large datasets at fine spatial and temporal resolutions will provide the foundation for training complex models. For example, a network of *Pondi* units can provide spatially and temporally explicit data to understand complex dynamics in a system. By integrating ground-based measurements with remote sensing technologies, such as drones or satellites, scalable IoT solutions like *Pondi* can unlock transformative insights into ecosystem dynamics, enabling advancements in agricultural productivity, environmental man-

agement, and climate resilience at regional and global scales (Shafi et al., 2020; Rajak et al., 2023).

Improving our ability to monitor and predict GHG dynamics can attract private sector investment to advance climate goals (Bellassen et al., 2015). For example, IoT devices can reduce uncertainty and operational costs in carbon projects, offering a robust and transparent system for measurement, reporting, and verification (MRV). This technological approach has the potential to strengthen global carbon credit markets and accelerate climate change mitigation efforts. In

addition to carbon monitoring, devices like the *Pondi* can be expanded to include passive acoustic sensors to monitor biodiversity through sound. Using AI-based species recognition algorithms, it is possible to automatically identify birds, frogs, and other vocal fauna, enabling scalable, long-term biodiversity assessments (Pérez-Granados, 2023; Höchst et al., 2022). Integrating AI-driven acoustic biodiversity monitoring with GHG flux data could support the development of joint biodiversity and carbon credit systems, allowing land managers to demonstrate measurable co-benefits of ecological restoration for both climate and nature (Bell and Malerba, 2025).

*Data availability.* All data and Gerber files for the printed circuit board will be available upon request.

*Author contributions.* MEM and PIM conceptualised the research. BE, MEM, AG, and PP developed the *Pondi*. LS, OO, JG, RK, and PP collected and analysed the data and helped with optimising the *Pondi* design. MEM wrote the first draft. All authors contributed to the final draft.

*Competing interests.* The contact author has declared that none of the authors has any competing interests.

*Review statement.* This paper was edited by Jack Middelburg and reviewed by Guillem Domenech-Gil and Gerard Rocher-Ros.

## References

Bastviken, D., Nygren, J., Schenk, J., Parellada Massana, R., and Duc, N. T.: Technical note: Facilitating the use of low-cost methane ($CH_4$) sensors in flux chambers – calibration, data processing, and an open-source make-it-yourself logger, Biogeosciences, 17, 3659–3667, https://doi.org/10.5194/bg-17-3659-2020, 2020.

Bell, K. and Malerba, M. E.: Biodiversity monitoring for biocredits: a case study comparing acoustic, eDNA, and traditional methods, Biodiversity and Conservation, 1–16, https://doi.org/10.1007/s10531-025-03083-0, 2025.

Bellassen, V., Stephan, N., Afriat, M., Alberola, E., Barker, A., Chang, J.-P., Chiquet, C., Cochran, I., Deheza, M., and Dimopoulos, C.: Monitoring, reporting and verifying emissions in the climate economy, Nature Climate Change, 5, 319–328, 2015.

Berthiaume, C., Cox, D., and Lugun, L.: An Improved and Robust Automated Greenhouse Gas Analyzer for Agricultural Fields, 2020.

Boesch, H., Liu, Y., Tamminen, J., Yang, D., Palmer, P. I., Lindqvist, H., Cai, Z., Che, K., Di Noia, A., and Feng, L.: Monitoring greenhouse gases from space, Remote Sensing, 13, 2700, https://doi.org/10.3390/rs13142700, 2021.

Bonetti, G., Trevathan-Tackett, S. M., Hebert, N., Carnell, P. E., and Macreadie, P. I.: Microbial community dynamics behind major release of methane in constructed wetlands, Applied Soil Ecology, 167, https://doi.org/10.1016/j.apsoil.2021.104163, 2021.

Borrego, C., Coutinho, M., Costa, A. M., Ginja, J., Ribeiro, C., Monteiro, A., Ribeiro, I., Valente, J., Amorim, J. H., Martins, H., Lopes, D., and Miranda, A. I.: Challenges for a New Air Quality Directive: The role of monitoring and modelling techniques, Urban Climate, 14, 328–341, https://doi.org/10.1016/j.uclim.2014.06.007, 2015.

Carey, R. O. and Migliaccio, K. W.: Contribution of wastewater treatment plant effluents to nutrient dynamics in aquatic systems: a review, Environ. Manage., 44, 205–217, 2009.

Curcoll, R., Morguí, J.-A., Kamnang, A., Cañas, L., Vargas, A., and Grossi, C.: Metrology for low-cost $CO_2$ sensors applications: the case of a steady-state through-flow (SS-TF) chamber for $CO_2$ fluxes observations, Atmos. Meas. Tech., 15, 2807–2818, https://doi.org/10.5194/amt-15-2807-2022, 2022.

Dalvai Ragnoli, M. and Singer, G.: The River Runner: a low-cost sensor prototype for continuous dissolved greenhouse gas measurements, J. Sens. Sens. Syst., 13, 41–61, https://doi.org/10.5194/jsss-13-41-2024, 2024.

Demanega, I., Mujan, I., Singer, B. C., Anđelković, A. S., Babich, F., and Licina, D.: Performance assessment of low-cost environmental monitors and single sensors under variable indoor air quality and thermal conditions, Building and Environment, 187, 107415, https://doi.org/10.1016/j.buildenv.2020.107415, 2021.

Dey, A.: Semiconductor metal oxide gas sensors: A review, Materials Science and Engineering: B, 229, 206–217, https://doi.org/10.1016/j.mseb.2017.12.036, 2018.

EPA: Inventory of U. S. Greenhouse Gas Emissions and Sinks: 1990–2021, U. S. Environmental Protection Agency, EPA 430-R-23-002, https://www.epa.gov/system/files/documents/2023-04/US-GHG-Inventory-2023-Main-Text.pdf (last access: 16 July 2025), 2023.

Eugster, W. and Kling, G. W.: Performance of a low-cost methane sensor for ambient concentration measurements in

preliminary studies, Atmos. Meas. Tech., 5, 1925–1934, https://doi.org/10.5194/amt-5-1925-2012, 2012.

Eugster, W., Laundre, J., Eugster, J., and Kling, G. W.: Long-term reliability of the Figaro TGS 2600 solid-state methane sensor under low-Arctic conditions at Toolik Lake, Alaska, Atmos. Meas. Tech., 13, 2681–2695, https://doi.org/10.5194/amt-13-2681-2020, 2020.

Grinham, A., Albert, S., Deering, N., Dunbabin, M., Bastviken, D., Sherman, B., Lovelock, C. E., and Evans, C. D.: The importance of small artificial water bodies as sources of methane emissions in Queensland, Australia, Hydrol. Earth Syst. Sci., 22, 5281–5298, https://doi.org/10.5194/hess-22-5281-2018, 2018.

Griscom, B. W., Adams, J., Ellis, P. W., Houghton, R. A., Lomax, G., Miteva, D. A., Schlesinger, W. H., Shoch, D., Siikamäki, J. V., and Smith, P.: Natural climate solutions, Proceedings of the National Academy of Sciences, 114, 11645–11650, 2017.

Harmon, T. C., Dierick, D., Trahan, N., Allen, M. F., Rundel, P. W., Oberbauer, S. F., Schwendenmann, L., and Zelikova, T. J.: Low-cost soil $CO_2$ efflux and point concentration sensing systems for terrestrial ecology applications, Methods in Ecology and Evolution, 6, 1358–1362, 2015.

Höchst, J., Bellafkir, H., Lampe, P., Vogelbacher, M., Mühling, M., Schneider, D., Lindner, K., Rösner, S., Schabo, D. G., and Farwig, N.: Bird@Edge: bird species recognition at the edge, International Conference on Networked Systems, 69–86, https://doi.org/10.1007/978-3-031-17436-0_6, 2022.

Hoffmann, M., Schulz-Hanke, M., Garcia Alba, J., Jurisch, N., Hagemann, U., Sachs, T., Sommer, M., and Augustin, J.: A simple calculation algorithm to separate high-resolution $CH_4$ flux measurements into ebullition- and diffusion-derived components, Atmos. Meas. Tech., 10, 109–118, https://doi.org/10.5194/amt-10-109-2017, 2017.

Holgerson, M. A. and Raymond, P. A.: Large contribution to inland water $CO_2$ and $CH_4$ emissions from very small ponds, Nature Geoscience, 9, 222–226, 2016.

Houghton, R. A., Byers, B., and Nassikas, A. A.: A role for tropical forests in stabilizing atmospheric $CO_2$, Nature Climate Change, 5, 1022–1023, 2015.

Hu, Z., Lee, J. W., Chandran, K., Kim, S., and Khanal, S. K.: Nitrous oxide ($N_2O$) emission from aquaculture: a review, Environmental Science & Technology, 46, 6470–6480, 2012.

IPCC: Climate change 2007: synthesis report. Contribution of working group I, II and III to the fourth assessment report of the intergovernmental panel on climate change, ISBN 92-9169-122-4, 2007.

IPCC: Summary for Policymakers, in: Climate Change 2023: Synthesis Report. Contribution of Working Groups I, II and III to the Sixth Assessment Report of the Intergovernmental Panel on Climate Change, edited by: Core Writing Team, Lee, H., and Romero, J., IPCC, Geneva, Switzerland, 1–34, https://doi.org/10.59327/IPCC/AR6-9789291691647.001, 2023.

Janssens-Maenhout, G., Pinty, B., Dowell, M., Zunker, H., Andersson, E., Balsamo, G., Bézy, J. L., Brunhes, T., Bösch, H., Bojkov, B., Brunner, D., Buchwitz, M., Crisp, D., Ciais, P., Counet, P., Dee, D., Denier van der Gon, H., Dolman, H., Drinkwater, M. R., Dubovik, O., Engelen, R., Fehr, T., Fernandez, V., Heimann, M., Holmlund, K., Houweling, S., Husband, R., Juvyns, O., Kentarchos, A., Landgraf, J., Lang, R., Löscher, A., Marshall, J., Meijer, Y., Nakajima, M., Palmer, P. I., Peylin, P., Rayner, P., Scholze, M., Sierk, B., Tamminen, J., and Veefkind, P.: Toward an Operational Anthropogenic $CO_2$ Emissions Monitoring and Verification Support Capacity, Bulletin of the American Meteorological Society, 101, E1439–E1451, https://doi.org/10.1175/bams-d-19-0017.1, 2020.

Kent, E. R., Bailey, S. K., Stephens, J., Horwath, W. R., and Paw U, K. T.: Measurements of greenhouse gas flux from composting green-waste using micrometeorological mass balance and flow-through chambers, Compost Science & Utilization, 27, 97–115, 2019.

Li, H., Guo, Y., Zhao, H., Wang, Y., and Chow, D.: Towards automated greenhouse: A state of the art review on greenhouse monitoring methods and technologies based on internet of things, Computers and Electronics in Agriculture, 191, 106558, https://doi.org/10.1016/j.compag.2021.106558, 2021a.

Li, Y., Shang, J., Zhang, C., Zhang, W., Niu, L., Wang, L., and Zhang, H.: The role of freshwater eutrophication in greenhouse gas emissions: A review, Sci. Total Environ., 768, 144582, https://doi.org/10.1016/j.scitotenv.2020.144582, 2021b.

Maher, D. T., Drexl, M., Tait, D. R., Johnston, S. G., and Jeffrey, L. C.: iAMES: An inexpensive, Automated Methane Ebullition Sensor, Environ. Sci. Technol., 53, 6420–6426, https://doi.org/10.1021/acs.est.9b01881, 2019.

Malerba, M. E., Wright, N., and Macreadie, P. I.: A continental-scale assessment of density, size, distribution and historical trends of farm dams using deep learning convolutional neural networks, Remote Sensing, 13, 319, https://doi.org/10.3390/rs13020319, 2021.

Malerba, M. E., de Kluyver, T., Wright, N., Schuster, L., and Macreadie, P. I.: Methane emissions from agricultural ponds are underestimated in national greenhouse gas inventories, Communications Earth & Environment, 3, 306, https://doi.org/10.1038/s43247-022-00638-9, 2022a.

Malerba, M. E., Friess, D. A., Peacock, M., Grinham, A., Taillardat, P., Rosentreter, J. A., Webb, J., Iram, N., Al-Haj, A. N., and Macreadie, P. I.: Methane and nitrous oxide emissions complicate the climate benefits of teal and blue carbon wetlands, One Earth, 5, 1336–1341, 2022b.

Malerba, M. E., Lindenmayer, D. B., Scheele, B. C., Waryszak, P., Yilmaz, I. N., Schuster, L., and Macreadie, P. I.: Fencing farm dams to exclude livestock halves methane emissions and improves water quality, Global Change Biology, https://doi.org/10.1111/gcb.16237, 2022c.

Martinsen, K. T., Kragh, T., and Sand-Jensen, K.: Technical note: A simple and cost-efficient automated floating chamber for continuous measurements of carbon dioxide gas flux on lakes, Biogeosciences, 15, 5565–5573, https://doi.org/10.5194/bg-15-5565-2018, 2018.

McGinn, S. M.: Measuring greenhouse gas emissions from point sources in agriculture, Canadian Journal of Soil Science, 86, 355–371, https://doi.org/10.4141/s05-099, 2006.

Morawska, L., Thai, P. K., Liu, X., Asumadu-Sakyi, A., Ayoko, G., Bartonova, A., Bedini, A., Chai, F., Christensen, B., Dunbabin, M., Gao, J., Hagler, G. S. W., Jayaratne, R., Kumar, P., Lau, A. K. H., Louie, P. K. K., Mazaheri, M., Ning, Z., Motta, N., Mullins, B., Rahman, M. M., Ristovski, Z., Shafiei, M., Tjondronegoro, D., Westerdahl, D., and Williams, R.: Applications of low-cost sensing technologies for air quality monitoring and exposure as-

sessment: How far have they gone?, Environ. Int., 116, 286–299, https://doi.org/10.1016/j.envint.2018.04.018, 2018.

Naslund, L. C., Mehring, A. S., Rosemond, A. D., and Wenger, S. J.: Toward more accurate estimates of carbon emissions from small reservoirs, Limnology and Oceanography, https://doi.org/10.1002/lno.12577, 2024.

Nguyen, T. K. L., Ngo, H. H., Guo, W., Chang, S. W., Nguyen, D. D., Nghiem, L. D., Liu, Y., Ni, B., and Hai, F. I.: Insight into greenhouse gases emissions from the two popular treatment technologies in municipal wastewater treatment processes, Sci. Total Environ., 671, 1302–1313, 2019.

Odebiri, O., Archbold, J., Glen, J., Macreadie, P. I., and Malerba, M. E.: Excluding livestock access to farm dams reduces methane emissions and boosts water quality, Science of The Total Environment, 175420, https://doi.org/10.1016/j.scitotenv.2024.175420, 2024.

Ollivier, Q. R., Maher, D. T., Pitfield, C., and Macreadie, P. I.: Punching above their weight: Large release of greenhouse gases from small agricultural dams, Glob. Chang. Biol., 25, 721–732, https://doi.org/10.1111/gcb.14477, 2018.

Ollivier, Q. R., Maher, D. T., Pitfield, C., and Macreadie, P. I.: Winter emissions of $CO_2$, $CH_4$, and $N_2O$ from temperate agricultural dams: fluxes, sources, and processes, Ecosphere, 10, https://doi.org/10.1002/ecs2.2914, 2019.

Pérez-Granados, C.: BirdNET: applications, performance, pitfalls and future opportunities, Ibis, 165, 1068–1075, 2023.

Pigliautile, I., Marseglia, G., and Pisello, A. L.: Investigation of $CO_2$ Variation and Mapping Through Wearable Sensing Techniques for Measuring Pedestrians' Exposure in Urban Areas, Sustainability, 12, https://doi.org/10.3390/su12093936, 2020.

Rajak, P., Ganguly, A., Adhikary, S., and Bhattacharya, S.: Internet of Things and smart sensors in agriculture: Scopes and challenges, Journal of Agriculture and Food Research, 14, 100776, https://doi.org/10.1016/j.jafr.2023.100776, 2023.

Rodrigues, C. I. D., Brito, L. M., and Nunes, L. J.: Soil carbon sequestration in the context of climate change mitigation: A review, Soil Systems, 7, 64, https://doi.org/10.3390/soilsystems7030064, 2023.

Rodríguez-García, V. G., Palma-Gallardo, L. O., Silva-Olmedo, F., and Thalasso, F.: A simple and low-cost open dynamic chamber for the versatile determination of methane emissions from aquatic surfaces, Limnology and Oceanography: Methods, https://doi.org/10.1002/lom3.10584, 2023.

Rosentreter, J. A., Borges, A. V., Deemer, B. R., Holgerson, M. A., Liu, S., Song, C., Melack, J., Raymond, P. A., Duarte, C. M., Allen, G. H., Olefeldt, D., Poulter, B., Battin, T. I., and Eyre, B. D.: Half of global methane emissions come from highly variable aquatic ecosystem sources, Nature Geoscience, 14, 225–230, https://doi.org/10.1038/s41561-021-00715-2, 2021.

Salam, A.: Internet of things for environmental sustainability and climate change, in: Internet of Things for sustainable community development: Wireless communications, sensing, and systems, Springer, 33–69, https://doi.org/10.1007/978-3-031-62162-8_2, 2024.

Saunois, M., Martinez, A., Poulter, B., Zhang, Z., Raymond, P. A., Regnier, P., Canadell, J. G., Jackson, R. B., Patra, P. K., Bousquet, P., Ciais, P., Dlugokencky, E. J., Lan, X., Allen, G. H., Bastviken, D., Beerling, D. J., Belikov, D. A., Blake, D. R., Castaldi, S., Crippa, M., Deemer, B. R., Dennison, F., Etiope, G.,

Gedney, N., Höglund-Isaksson, L., Holgerson, M. A., Hopcroft, P. O., Hugelius, G., Ito, A., Jain, A. K., Janardanan, R., Johnson, M. S., Kleinen, T., Krummel, P. B., Lauerwald, R., Li, T., Liu, X., McDonald, K. C., Melton, J. R., Mühle, J., Müller, J., Murguia-Flores, F., Niwa, Y., Noce, S., Pan, S., Parker, R. J., Peng, C., Ramonet, M., Riley, W. J., Rocher-Ros, G., Rosentreter, J. A., Sasakawa, M., Segers, A., Smith, S. J., Stanley, E. H., Thanwerdas, J., Tian, H., Tsuruta, A., Tubiello, F. N., Weber, T. S., van der Werf, G. R., Worthy, D. E. J., Xi, Y., Yoshida, Y., Zhang, W., Zheng, B., Zhu, Q., Zhu, Q., and Zhuang, Q.: Global Methane Budget 2000–2020, Earth Syst. Sci. Data, 17, 1873–1958, https://doi.org/10.5194/essd-17-1873-2025, 2025.

Schuster, L., Taillardat, P., Macreadie, P. I., and Malerba, M. E.: Freshwater wetland restoration and conservation are long-term natural climate solutions, Science of the Total Environment, 922, 171218, https://doi.org/10.1016/j.scitotenv.2024.171218, 2024.

Shafi, U., Mumtaz, R., Iqbal, N., Zaidi, S. M. H., Zaidi, S. A. R., Hussain, I., and Mahmood, Z.: A multi-modal approach for crop health mapping using low altitude remote sensing, internet of things (IoT) and machine learning, IEEE Access, 8, 112708–112724, 2020.

Shah, A., Laurent, O., Lienhardt, L., Broquet, G., Rivera Martinez, R., Allegrini, E., and Ciais, P.: Characterising the methane gas and environmental response of the Figaro Taguchi Gas Sensor (TGS) 2611-E00, Atmos. Meas. Tech., 16, 3391–3419, https://doi.org/10.5194/amt-16-3391-2023, 2023.

Sieczko, A. K., Duc, N. T., Schenk, J., Pajala, G., Rudberg, D., Sawakuchi, H. O., and Bastviken, D.: Diel variability of methane emissions from lakes, Proceedings of the National Academy of Sciences, 117, 21488–21494, 2020.

Smith, P., Bustamante, M., Ahammad, H., Clark, H., Dong, H., Elsiddig, E. A., Haberl, H., Harper, R., House, J., and Jafari, M.: Agriculture, forestry and other land use (AFOLU), in: Climate change 2014: mitigation of climate change. Contribution of Working Group III to the Fifth Assessment Report of the Intergovernmental Panel on Climate Change, Cambridge University Press, 811–922, https://doi.org/10.1017/CBO9781107415416.017, 2014.

Sø, J. S., Sand-Jensen, K., and Kragh, T.: Self-Made Equipment for Automatic Methane Diffusion and Ebullition Measurements From Aquatic Environments, Journal of Geophysical Research: Biogeosciences, 129, https://doi.org/10.1029/2024jg008035, 2024.

Thakur, I. S. and Medhi, K.: Nitrification and denitrification processes for mitigation of nitrous oxide from waste water treatment plants for biovalorization: Challenges and opportunities, Bioresource Technology, 282, 502–513, 2019.

Thanh Duc, N., Silverstein, S., Wik, M., Crill, P., Bastviken, D., and Varner, R. K.: Technical note: Greenhouse gas flux studies: an automated online system for gas emission measurements in aquatic environments, Hydrol. Earth Syst. Sci., 24, 3417–3430, https://doi.org/10.5194/hess-24-3417-2020, 2020.

UN Environment Programme: Emissions Gap Report 2023: Broken Record – Temperatures hit new highs, yet world fails to cut emissions (again). Nairobi, https://doi.org/10.59117/20.500.11822/43922, 2023.

van den Bossche, M., Rose, N. T., and De Wekker, S. F. J.: Potential of a low-cost gas sensor for atmospheric methane monitoring, Sensors and Actuators B: Chemical, 238, 501–509, 2017.

Varadharajan, C. and Hemond, H. F.: Time-series analysis of high-resolution ebullition fluxes from a stratified, freshwater lake, Journal of Geophysical Research: Biogeosciences, 117, https://doi.org/10.1029/2011JG001866, 2012.

Watkins, T.: Draft roadmap for next generation air monitoring, Environmental Protection Agency, 2, 2013.

Webb, J. R., Santos, I. R., Maher, D. T., and Finlay, K.: The importance of aquatic carbon fluxes in net ecosystem carbon budgets: A catchment-scale review, Ecosystems, 22, 508–527, 2019.

Wu, H., Cui, H., Fu, C., Li, R., Qi, F., Liu, Z., Yang, G., Xiao, K., and Qiao, M.: Unveiling the crucial role of soil microorganisms in carbon cycling: A review, Science of The Total Environment, 168627, https://doi.org/10.1016/j.scitotenv.2023.168627, 2023.